Supplementary Information

Increasing flow velocity promotes nitrification and denitrification in benthic biofilms via enhancing the diversity and potential predation-prey among multi-trophic microorganisms

Bo Zhang[1], Juan Chen[1]*, Chao Wang[1], Peifang Wang[1], Ge Cui[1], Han Gao[1], Bingbing Feng[1], Sheng Sheng[2], Jingjing Fu[2]

1. Key Laboratory of Integrated Regulation and Resource Department on Shallow Lakes, Ministry of Education, College of Environment, Hohai University, Nanjing 210098, China

2. PowerChina Huadong Engineering Corporation Limited, Hangzhou 311122, China

* **Corresponding Author**

Address: College of Environment, Hohai University, Xikang Road No.1 Nanjing 210098, China

Telephone: +86-025-83787930; Fax: +86-025-83787332

E-mail address: chenjuanmn@hhu.edu.cn

Main contents: Figures S1-S12; Tables S1-S3

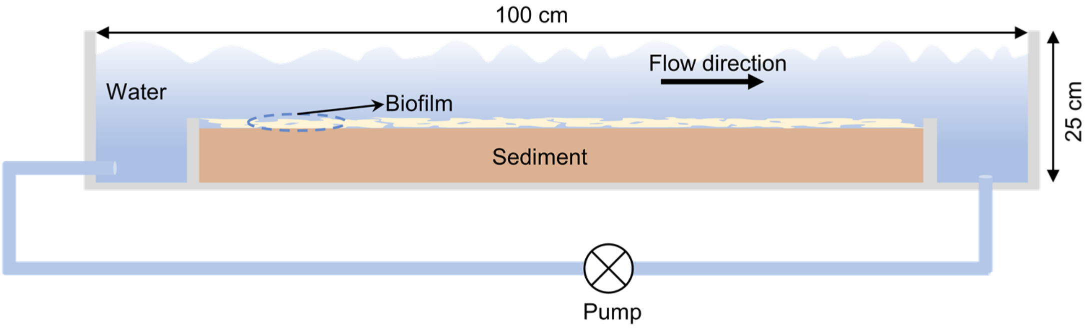

Fig. S1 Structure diagram of the experimental channel.

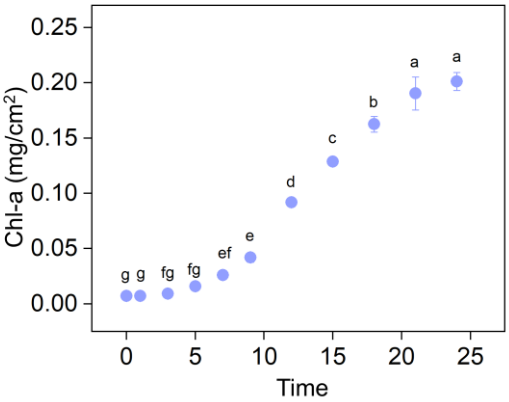

Fig. S2 Changes of chlorophyll-a (Chl-a) content of benthic biofilms over 24 days (at each sampling time, means with different letters are significant differences at $p < 0.05$ according to one-way ANOVA).

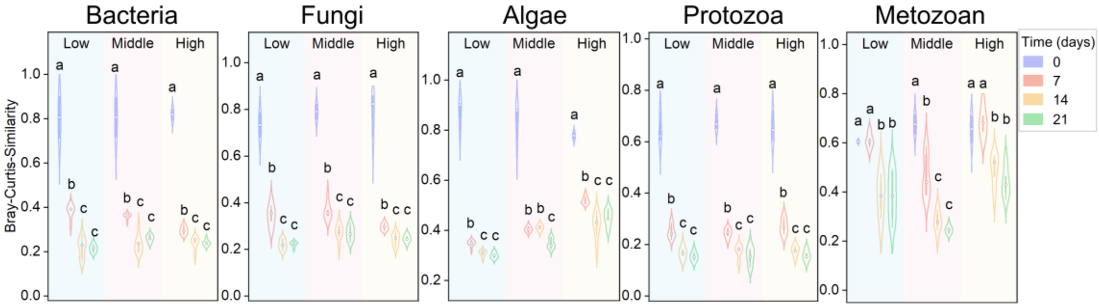

Fig. S3 The similarity of bacterial, fungal, algal, protozoan and metazoan communities between time points in each flow velocity condition (at each sampling time, means with different letters are significant differences at $p < 0.05$ according to one-way ANOVA).

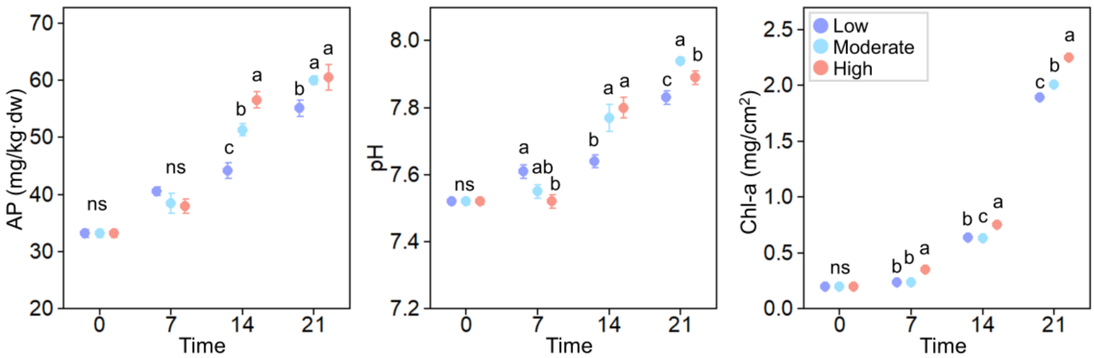

Fig. S4 Changes in the chemical properties of the benthic biofilm under different flow velocity conditions during the 21-day experiment (at each sampling time, means with different letters are significant differences at $p < 0.05$ according to one-way ANOVA; ns: not significant, AP: available phosphorus, Chl-a: chlorophyll-a).

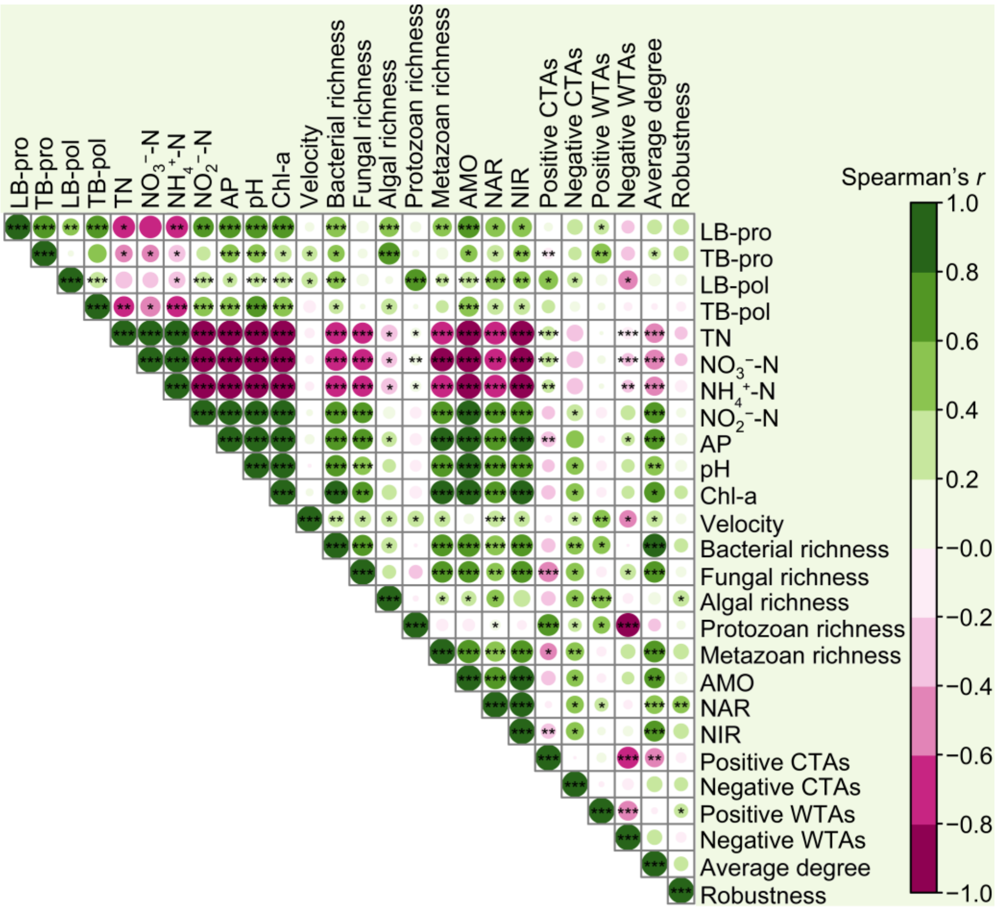

Fig. S5 Spearman's correlations between chemical properties and the diversity of microbes at different trophic levels in the benthic biofilms under different flow velocity conditions (colors gradient in the circle represents the Spearman's *r* value; *, ** and *** indicate significant Spearman's correlations at $p < 0.05$, $p < 0.01$ and $p < 0.001$, respectively; TB-pol: polysaccharides of tightly bound EPS, TB-pro: protein of tightly bound EPS, LB-pol: polysaccharides of lightly bound EPS, LB-pro: protein of lightly bound EPS, Chl-a: chlorophyll-a, NO_3^--N: nitrate-nitrogen, NO_2^--N: nitrite-nitrogen, NH_4^+-N: ammonia-nitrogen, TN: total nitrogen, AP: available phosphorus, CTAs: cross-trophic associations; WTAs: within trophic associations, AMO: ammonia monooxygenase, NIR: nitrite reductase, NAR: nitrate reductase).

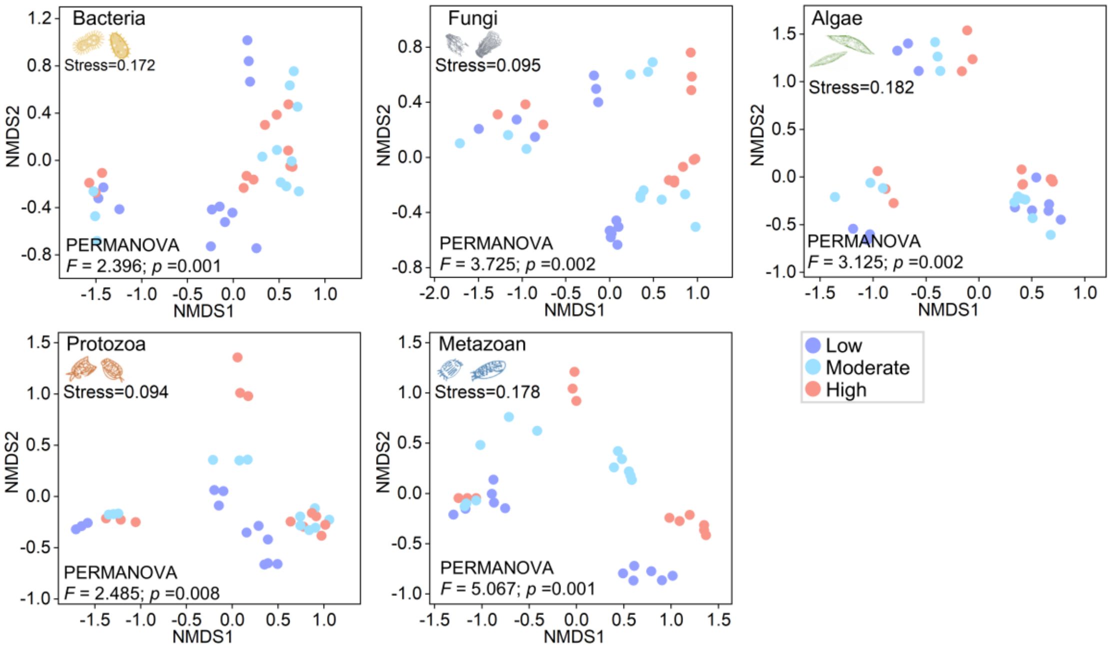

Fig. S6 Non-metric multidimensional scaling (NMDS) plot of bacterial, fungal, algal, protozoan, and metazoan communities in the benthic biofilms under different flow velocity conditions.

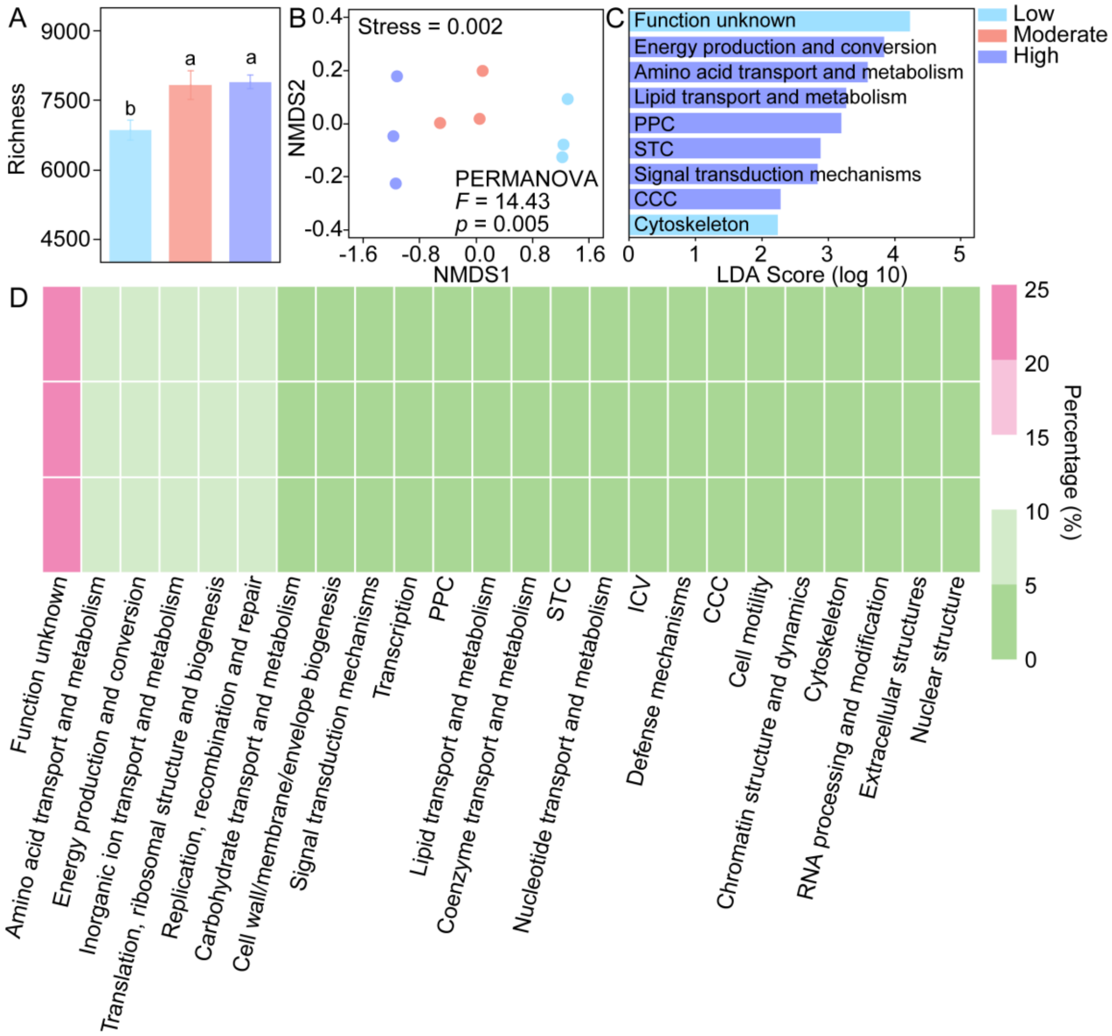

Fig. S7 The richness index of KOs (KEGG orthologs) (A), NMDS of KOs in different flow velocities for benthic biofilms (B), significantly enriched pathway of COG (clustering orthologous group) annotation in different flow velocities representing marked functions (C, $p < 0.05$), percentage of functional categories of benthic biofilm samples according to the EggNOG database (D) (at each sampling time, means with different letters are significant differences at $p < 0.05$ according to one-way ANOVA; PPC: posttranslational modification, protein turnover, chaperones, STC: secondary metabolites biosynthesis, transport and catabolism, ICV: intracellular trafficking, secretion, and vesicular transport, CCC: cell cycle control, cell division, chromosome partitioning).

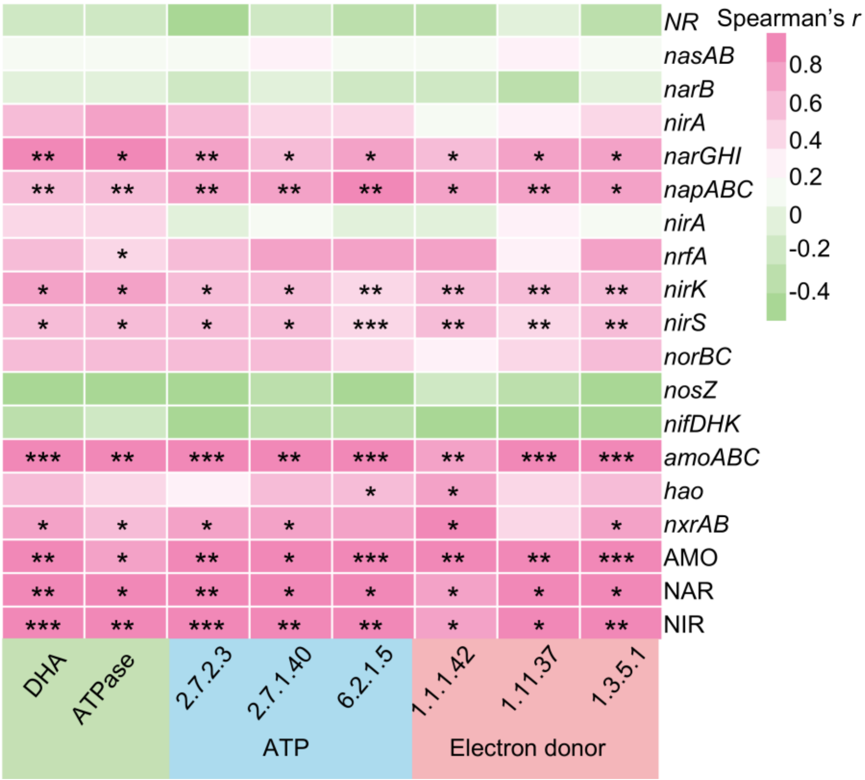

Fig. S8 Spearman's analysis between the relative abundances of nitrogen cycling-related genes, the activities of dehydrogenase (DHA) and ATP synthase (ATPase), ammonia monooxygenase (AMO), nitrate reductase (NAR) and nitrite reductase (NIR) and the relative abundance of genes encoding ATP and electron donor production-related enzymes (phosphoglycerate kinase (2.7.2.3), pyruvate kinase (2.7.1.40), succinyl-CoA synthase (6.2.1.5), isocitrate dehydrogenase (1.1.1.42), malate dehydrogenase (1.1.1.37), and succinate dehydrogenase (1.3.5.1); *, ** and *** indicate significant Spearman's correlations at $p < 0.05$, $p < 0.01$ and $p < 0.001$, respectively).

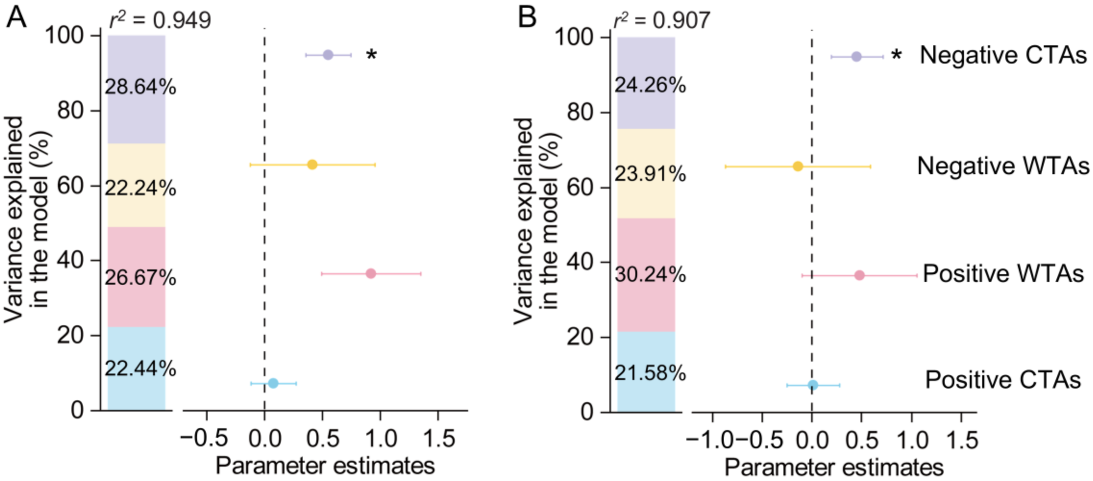

Fig. S9 Multiple regression analysis revealing the relative effect of multi-trophic microorganism associations on the relative abundances of encoding synthetic energy (A) and electron donor (B) genes (CTAs: cross-trophic associations, WTAs: within trophic associations; * and ** indicate significant linear correlations at $p < 0.05$ and $p < 0.01$).

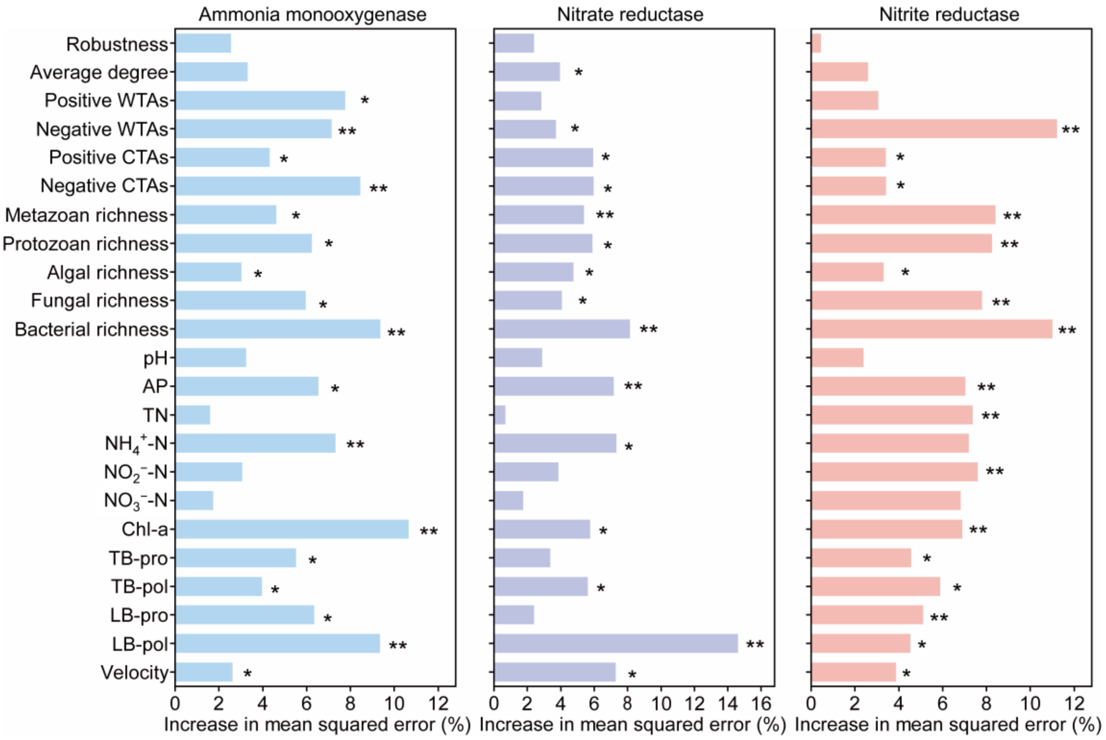

Fig. S10 The important factors affecting the ammonia monooxygenase, nitrate reductase and nitrite reductase activities identified by random forest model (TB-pol: polysaccharides of tightly bound EPS, TB-pro: protein of tightly bound EPS, LB-pol: polysaccharides of lightly bound EPS, LB-pro: protein of lightly bound EPS, Chl-a: chlorophyll-a, NO_3^--N: nitrate-nitrogen, NO_2^--N: nitrite-nitrogen, NH_4^+-N: ammonia-nitrogen, TN: total nitrogen, AP: available phosphorus, CTAs: cross-trophic associations, WTAs: within trophic associations; * and ** indicate significant correlations at $p < 0.05$ and $p < 0.01$, respectively).

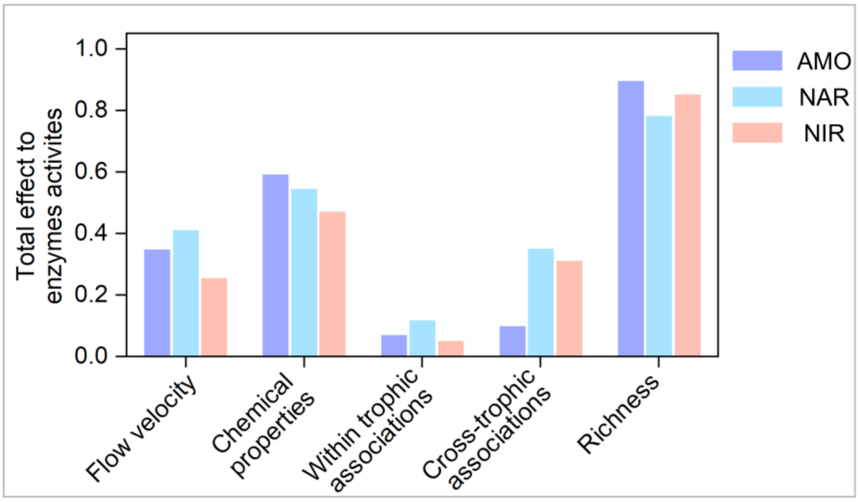

Fig. S11 Partial least squares path modeling analysis the standardized effects of factors on activities of ammonia monooxygenase (AMO), nitrate reductase (NAR) and nitrite reductase (NIR).

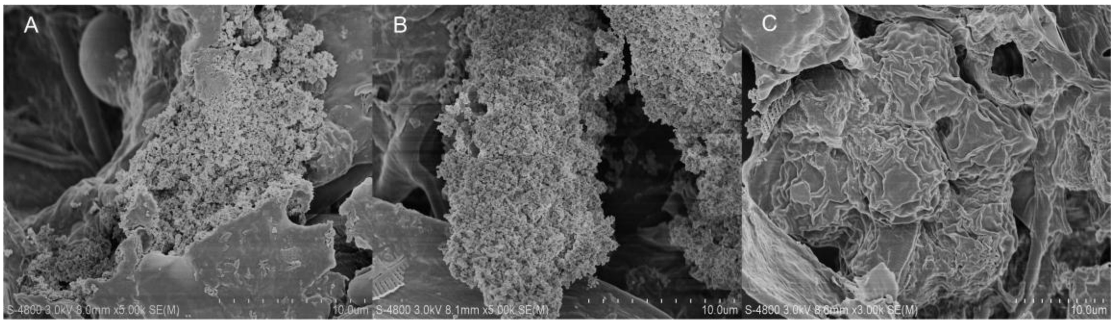

Fig. S12 Images of scanning electron microscopy of the benthic biofilms under low (A), moderate (B) and high (C) flow velocity conditions.

Table S1. The 10 sampling sites information along the Chu River.

Sampling site	**Longitude**	**Latitude**	**Velocity** (m/s)
S1	32°14’40” N	118°39‘58” E	0.156
S2	32°21’24” N	118°42’12” E	0.077
S3	32°19’11” N	118°41’28” E	0.068
S4	32°22’54” N	118°43’57” E	0.087
S5	32°21’22” N	118°45’44” E	0.058
S6	32°20’28” N	118°48’20” E	0.062
S7	32°19’35” N	118°50’25” E	0.047
S8	32°17’35” N	118°50’57” E	0.073
S9	32°14’41” N	118°52’53” E	0.116
S10	32°15’25” N	118°58’24” E	0.045

Table S2. Classification of potential microbial association among bacteria, fungi, algae, protozoa and metazoan.

Association types	**Potential microbial associations**
Positive within trophic	Bacteria ↔ Bacteria
	Algae ↔ Algae
	Fungi↔Fungi
	Protozoa ↔ Protozoa
	Metazoan ↔ Metazoan
	Algae ↔ Bacteria
	Algae ↔ Fungi
	Fungi ↔ Bacteria
Negative within trophic	Bacteria ↔ Bacteria
	Algae ↔ Algae
	Fungi↔Fungi
	Protozoa ↔ Protozoa
	Metazoan ↔ Metazoan
	Algae ↔ Bacteria
	Algae ↔ Fungi
	Fungi ↔ Bacteria
Positive cross-trophic	Metazoan ↔ Protozoa
	Metazoan ↔ Algae
	Metazoan ↔ Fungi
	Metazoan ↔ Bacteria
	Protozoa ↔ Algae
	Protozoa ↔ Fungi
	Protozoa ↔ Bacteria
Negative cross-trophic	Metazoan ↔ Protozoa
	Metazoan ↔ Algae
	Metazoan ↔ Fungi
	Metazoan ↔ Bacteria
	Protozoa ↔ Algae
	Protozoa ↔ Fungi
	Protozoa ↔ Bacteria
	Metazoan ↔ Protozoa

Table S3. Information of the functional genes involved in the glycolysis, tricarboxylic acid (TCA) cycle and electron transform system processes identified in Kyoto Encyclopedia of Genes and Genomes (KEGG) database.

Gene category	**Gene name**	**KEGG orthology number**	**Encoded protein (EC)**
Glycolysis	*HK*	K00844	2.7.1.1
	glk	K00845	2.7.1.2
	pfkC	K00918	2.7.1.147
	ADPGK	K08074	
	GPI	K01810	5.3.1.9
	pgi1	K06859	
	tal-pgi	K13810	
	pgo-pmi	K15916	
	pfkA	K00850	2.7.1.11
	pfkB	K16370	
	pfk	K21071	
	pfkC	K00918	2.7.1.146
	K01622	K01622	4.1.2.13
	ALDO	K01623	
	fbaA	K01624	
	fbaB	K11645	
	K16306	K16306	
	TPI	K01803	5.3.1.1
	gap2	K00150	1.2.1.59
	GAPDH	K00134	1.2.1.12
	GADPHS	K10705	
	PGK	K00927	2.7.2.3
	gmpl	K15633	5.4.2.12
	apgM	K15635	
	gpmA	K01834	5.4.2.11
	gpmB	K15634	
	ENO	K01689	4.2.1.11
	pyk	K00873	2.7.1.40
TCA cycle	*DLAT*	K00627	2.3.1.12
	PDHA	K00161	1.2.4.1
	PDHB	K00162	
	aceE	K00163	
	PC	K01958	6.4.1.1
	pycA	K01959	
	pycB	K01960	
	CS	K01647	2.3.3.1
	ACLY	K01648	2.3.3.8
	aclA	K15230	
	aclB	K15231	

	acnA	K01681	4.2.1.3
	acnB	K01682	
	IDH1	K00031	1.1.1.42
	DLD	K00382	1.8.1.4
	DLST	K00658	2.3.1.61
	kgd	K01616	
	sucD	K01902	6.2.1.5
	sucC	K01903	
	fumC	K01679	4.2.1.2
	fumB	K01678	
	fumA	K01677	
	fumAB	K01676	
	mdh	K00024	1.1.1.37
	MDH1	K00025	
	MDH2	K00026	